

RESEARCH PAPER

 OPEN ACCESS

## BLT2 expression improves skin integrity and protects from alterations caused by hyperglycemia in type 2 diabetes

Alberto Leguina-Ruzzi <sup>a</sup> and Juan P. Valderas <sup>b</sup>

<sup>a</sup>Juntendo University, School of Medicine, Tokyo, Japan; <sup>b</sup>Departamento de Ciencias Médicas, Facultad de Medicina Odontología, Universidad de Antofagasta, Antofagasta, Chile

### ABSTRACT

Type 2 diabetes (T2D) can go undiagnosed for years, leading to a stage where chronic high blood sugar produces complications such as delayed wound healing. Reports have shown that BLT2 activation improves keratinocyte migration and wound healing, as well as protecting the epidermal barrier through the promotion of actin polymerization.

The goal of this study was to elucidate the role of BLT2 expression in skin epithelial integrity in T2D.

For this purpose, we used both wild type (WT) and BLT2 knockout mice in a model, in which a T2D-like phenotype was induced by keeping the animals on a high fat (HF) diet over 5 weeks. In a parallel *in vitro* approach, we cultured BLT2-transfected HaCaT cells at both low and high glucose concentrations for 48 h. Structure, transepithelial resistance (TEER), IL-1 $\beta$ , IL-8 or CXCL2, MMP9, Filaggrin, Loricrin and Keratin 10 (K10) were evaluated *ex vivo* and *in vitro*. Additionally, wound healing (WH) was studied *in vitro*.

The skin from T2D and BLT2 knockout mice showed a reduction in TEER and the expression of IL-1 $\beta$ , and an increase in CXCL2, MMP9, Filaggrin, Loricrin and K10 expression. The structure suggested an atrophic epidermis; however, the skin was dramatically affected in the BLT2 knockout mice kept on a HF diet.

HaCaT-BLT2 cells presented as an organized monolayer and showed higher TEER and wound healing compared with vector only-transfected HaCaT-Mock cells. Likewise, alterations in the expression of skin inflammatory, matrix degradation and differentiation markers under low and high glucose conditions were less severe than in HaCaT-Mock cells.

Our results suggest that BLT2 improves epithelial integrity and function by regulating differentiation markers, cytokines and MMP9. Furthermore, BLT2 attenuates the damaging effects of high glucose levels, thereby accelerating wound healing.

### ARTICLE HISTORY

Received 1 November 2016  
Accepted 28 November 2016

### KEYWORDS


BLT2; epithelium;  
hyperglycemia; skin barrier  
integrity; skin ulcer; type 2  
diabetes


## Introduction

Type 2 diabetes (T2D) is a metabolic disease affecting over 340 million people worldwide.<sup>1</sup> It is characterized by a cellular inability to respond to insulin, often referred to as insulin resistance, leading to chronic hyperglycemia.<sup>2</sup> T2D can go undiagnosed and even unnoticed for years; during this time, the patient's initially normal response to a high blood glucose level - i.e., the secretion of insulin and the subsequent cellular uptake of glucose, resulting in lowered glucose levels - is gradually impaired. This process finally leads to a stage where a permanently elevated high blood sugar level produces symptoms in the

patient, including delayed wound healing caused by chronic inflammation.<sup>3</sup> This can result in skin complications and the risk of amputation, both of which are most prevalent in the elderly. In particular, the difficulties associated with the management of foot ulceration are a factor which increases morbidity and mortality in this age group.<sup>4</sup>

Leukotriene B<sub>4</sub> (LTB<sub>4</sub>) receptor type 2 (BLT2) is a G-protein-coupled receptor (GPCR), which binds to LTB<sub>4</sub> and 12(S)-hydroxyheptadeca-5Z,8E,10E-trienoic acid (12-HHT).<sup>5,6</sup> It is mainly expressed in epithelial cells, such as epidermal keratinocytes<sup>7</sup> and intestinal

**CONTACT** Alberto Leguina-Ruzzi  [alberto@juntendo.ac.jp](mailto:alberto@juntendo.ac.jp)  Juntendo University, School of Medicine, Tokyo, Japan, Hongo 2-1-1, Bunkyo-ku, Tokyo 113-8421, Japan.

 Supplemental data for this article can be accessed on the [publisher's website](#).

© 2017 Alberto Leguina-Ruzzi and Juan P. Valderas. Published with license by Taylor & Francis.

This is an Open Access article distributed under the terms of the Creative Commons Attribution-NonCommercial-NoDerivatives License (<http://creativecommons.org/licenses/by-nc-nd/4.0/>), which permits non-commercial re-use, distribution, and reproduction in any medium, provided the original work is properly cited, and is not altered, transformed, or built upon in any way.

epithelial cells.<sup>8</sup> Research on BLT2-deficient mice and studies of BLT2 antagonists have implicated the receptor in skin wound healing<sup>7</sup> and carcinogenesis,<sup>9,10</sup> as well as in the pathogenesis of arthritis<sup>11</sup> and bronchial asthma.<sup>12–14</sup> In line with this, BLT2-deficient mice presented with a more severe phenotype compared with wild type mice in a dextran sodium sulfate (DSS)-induced colitis model.<sup>14</sup>

Several recent findings are building a picture of BLT2 as an important player in skin barrier function and wound healing. BLT2 has been implicated in the regulation of tight junction proteins,<sup>15</sup> as well as in actin polymerization<sup>16</sup>; both of these processes are central to enhancing skin barrier function.<sup>15</sup> In addition, pharmacological activation of the BLT2 receptor has been found to promote keratinocyte migration, thereby enhancing fibroblast proliferation and improving wound healing in a model of type 1 diabetes.<sup>17</sup>

However, to date, there are no studies showing the effect of BLT2 expression on skin integrity in the context of T2D, as well as its relation with markers of inflammation, matrix degradation and differentiation as mediators of the regulatory process.

Since keratinocytes are both the predominant epidermal cell type responsible for skin repair and highly susceptible to damage,<sup>18</sup> the study of these cells is well suited to investigate the participation of BLT2 in the physiopathology of T2D hyperglycemia. The present study aims to evaluate the hypothesis that the BLT2 receptor expressed by keratinocytes acts a regenerative receptor, which promotes tissue injury healing and maintains integrity of the skin barrier by protecting it from the damaging effects of chronic hyperglycemia.

## Materials and methods

### Animal model of type 2 diabetes

BLT2 knockout (*Ltb4r2*<sup>-/-</sup>) mice were generated as previously described<sup>19–21</sup> and backcrossed to strain C57BL/6J for >12 generations. In all experiments, male mice of 7–21 weeks of age were used. All mice were kept in a 12h light: 12h dark cycle in a specific pathogen-free barrier facility. The study protocol was approved by the Ethics Committee for Animal Experimentation at Juntendo University, Japan.

10 wild type (WT) and 10 BLT2 knockout mice were mixed to form 2 groups of 10 animals each. One was fed a low fat chow (LF) (D12450B 35 kcal% fat) as a control. The second group was kept on a high fat (HF) diet

(D12492, 60 kcal% fat). Weight was controlled weekly after 4 hours of fasting. All mice were male and 21 weeks old at the start of the dietary regime.

### Glucose tolerance test, triglycerides and cholesterol measurement

A 100  $\mu$ L blood sample was obtained from the tail vein after 6 hours of fasting for triglyceride and cholesterol levels were measurement. After intraperitoneal (IP) injection with 1 g/kg of D-Glucose (Sigma-Aldrich, catalog no. G8644), glucose levels were measured at 15, 30, 60, 90, and 120 minutes. All the parameters were examined using the portable CardioChek<sup>®</sup> PA (CardioChek<sup>®</sup>, catalog no. 0197) device and the compatible PTS Panel<sup>®</sup> test strips.

### Insulin ELISA

Blood samples of 500  $\mu$ L were obtained from the tail vein of the animals and kept at room temperature for 30 minutes. After coagulation, the samples were centrifuged for 20 minutes to obtain the serum. Insulin levels were measured using the Insulin Ultrasensitive Mouse ELISA kit (Merckodia, article no. 10-1249-01).

### Homeostatic model assessment

Homeostatic model assessments of insulin resistance (HOMA-IR) and  $\beta$ -cell function (HOMA- $\beta$ ) were calculated based on the following formulas:

$$\text{HOMA-IR} = \frac{\text{serum glucose (mg / dL)} \times \text{plasma insulin}(\mu\text{U / mL})}{405}$$

$$\text{HOMA-}\beta = \frac{360 \times \text{plasma insulin}(\mu\text{U / mL})}{\text{serum glucose(mg / dL)} - 63\%}$$

### Histology

After harvesting, skin samples were fixed in 10% formalin, paraffin-embedded, and stained with hematoxylin and eosin (HE) for reference, and with Masson's trichrome stain (MT). Images were taken using a Keyence BZ-9000 fluorescence microscope in visible light.

Histological analysis and epidermal thickness quantification were performed blinded to the experimental conditions in 3 sections per animal and 2 slides per sample. An average was calculated for the graphic.

### Reverse transcription and quantitative PCR

Total RNA was extracted in 2 ways: for whole skin, the RNeasy<sup>®</sup> Fibrous Tissue Mini Kit (QIAGEN, catalog no. 74704) was used; RNA from cells was extracted by a guanidinium thiocyanate-phenol-chloroform extraction using TRIzol<sup>®</sup> (Life Technologies/Thermo Fisher Scientific, catalog no. 15596018). Reverse transcription was performed using 2  $\mu$ g of total RNA. Quantitative PCR was performed on 2.5  $\mu$ l reverse-transcribed product from the previous step, using the FastStart Essential DNA Green Master Mix (Roche, catalog no. 06402712001). Primer sequences were as follows: Murine IL-1 $\beta$  (IL1b)

FW 5'-TCCAGGATGAGGACATGAGCAC-3'  
 RV 5'-GAACGTCACACACCAGCAGGTTA-3'  
 Murine CXCL2 (Cxcl2)  
 FW 5'-CGCTGTCAATGCCTGAAG-3'  
 RV 5'-GGCGTCACACTCAAGCTCT-3'  
 Murine MMP9 (Mmp9)  
 FW 5'-CCTACTCTGCCTGCACCACTAAA-3'  
 RV 5'-CTGCTTGCCAGGAAGACGAA-3'  
 Murine filaggrin (Flg)  
 FW 5'-GAAGGAACTTCTGGAAGGACAAC-3'  
 RV 5'-TCCATCAGTCCACCATGCCTC-3'  
 Murine loridin (Lor)  
 FW 5'-TCCTATGGAGGTGGTTCAG-3'  
 RV 5'-CCACCTCCGAGTACTTGAC-3'  
 Murine keratin 10 (Krt10)  
 FW 5'-CGGTGGAGGTGGCAGCTTCGG-3'  
 RV 5'-CTCGCTGGCTTGAGTTGCCATGCTT-3'  
 Murine  $\beta$ -actin (actb)  
 FW 5'-CATCCGTAAGACCTCTATGCCAAC-3'  
 RV 5'-ATGGAGCCACCGATCCACA-3'  
 Human IL-1 $\beta$  (IL1B)  
 FW 5'-GCCCTAACAGATGAAGTGCTC-3'  
 RV 5'-GAACCAGCATCTTCCTCAG-3'  
 Human IL-8 (IL8)  
 FW 5'-CGGAAGGAACCATCTCACTG-3'  
 RV 5'-AGCACTCCTTGCCAAAAGT-3'  
 Human MMP9 (MMP9)  
 FW 5'-GACGCAGACATCGTCATCCAGTTT-3'  
 RV 5'-GCCGCGCCATCTGCGTTT-3'  
 Human filaggrin (FLG)  
 FW 5'-GCAAGGTCAAGTCCAGGAGAA-3'  
 RV 5'-CCCTCGGTTTCCACTGTCTC-3'  
 Human loridin (LOR)  
 FW 5'-GTGGGAGCGTCAAGTACTCC-3'  
 RV 5'-TAGAGACGCCTCCGTAGCTC-3'

Human keratin 10 (KRT10)

FW 5'- TGGTTCAATGAAAAGAGCAAGGA-3'  
 RV 5'-GGGATTGTTTCAAGGCCAGTT-3'  
 Human  $\beta$ -actin (ACTB)  
 FW 5'-TGGCACCCAGCACAAATGAA-3'  
 RV 5'-CTAAGTCATAGTCCGCCTAGAAGCA-3'

PCR was performed with an initial denaturation at 95°C for 20 s, followed by 45 cycles of 95°C for 3 s and 60°C for 30 s in a LightCycler<sup>®</sup> 96 (Roche, catalog no. 33863). Gene expression levels were calculated using the  $\Delta\Delta$ Ct method. Expression levels of the standard house-keeping gene  $\beta$ -actin were used for normalization.

### Cell culture

HaCaT cells were transfected with a FLAG-tagged human BLT2-pCXN2.1 vector, or with the empty pCXN2.1 vector as a control. Stable transfectants were selected in the presence of 1 mg/ml G418 (Wako Pure Chemical Industries, catalog no. 071-06431) and incubated with an anti-FLAG antibody (2H8),<sup>22</sup> followed by an Alexa Fluor 488-conjugated goat anti-mouse IgG secondary antibody (Life Technologies, A-11001). Immortalized human HaCaT keratinocytes were maintained in D-MEM (Wako Pure Chemical Industries, catalog no. 044-29765) containing 10% Gibco<sup>®</sup> FBS (Thermo Fisher Scientific, catalog no. 16000-069). For the low glucose treatment, the medium was changed to D-MEM containing 5 mM glucose (Wako Pure Chemical Industries, catalog no. 041-29775); for the high glucose treatment keratinocytes were maintained in D-MEM 25 mM glucose (Wako Pure Chemical Industries, 044-29765) and in both conditions the cells were treated without FBS.

### In vitro scratch assay

HaCaT cells (1.5  $\times$  10<sup>4</sup> cells/well) were seeded onto a collagen I-coated 96-well IncuCyte<sup>™</sup> ImageLock<sup>™</sup> tissue culture plate (Essen BioScience, catalog no. 4379) and incubated in a standard CO<sub>2</sub> incubator for 48 h to form a cell monolayer, before being treated with 2  $\mu$ g/mL Mitomycin C (Sigma-Aldrich, catalog no. M0503) for 2 h. Wounds were made with the 96-well WoundMaker<sup>™</sup> (Essen BioScience, 4493). In order to remove any detached cells, wounded cell layers were washed twice with culture medium before treatment with 100  $\mu$ l of medium containing the appropriate glucose concentrations. Images of the wounds were automatically acquired within the CO<sub>2</sub> incubator using

the IncuCyte™ ZOOM software package (Essen BioScience, catalog no. 2016A). Typical kinetic updates were taken at 3 h intervals for the duration of the experiment. Finally, cell confluence analysis was performed using the IncuCyte™ ZOOM software.

### **Phallotoxin staining**

50000 cells were seeded in collagen I-coated glass bottom plates and left to settle overnight before being incubated with the different glucose concentrations for 48 h. After incubation, the cells were washed once with 1x PBS and fixed with 4% paraformaldehyde for 10 minutes at room temperature before being washed again with 1x PBS. Following permeabilization with 0.01% Triton® X-100 (Nacalai, catalog no. 9002-93-1) for 3 minutes the cells were again washed with 1x PBS. Finally, 200  $\mu$ L of a 1:250 dilution of Alexa Fluor 488® Phalloidin (Thermo Fisher Scientific, A12379) were pipetted over the cells, which were then left to incubate for 20 minutes, washed twice with 1x PBS, and mounted with VECTASHIELD antifade mounting medium with DAPI (Vector Laboratories, catalog no. H-1200) onto 18 mm square glasses. The slides were visualized using a Leica TCS SP5 confocal laser microscope.

### **Transepithelial electrical resistance (TEER) measurement**

Ex vivo TEER measurement was performed using a modification of the protocol described in reference.<sup>23</sup> Skin samples with a diameter of 8 mm and a thickness of 1 mm were obtained from the back of the animal using disposable biopsy punches (Kai Medical, catalog no. BP-80F) and placed onto a 0.4  $\mu$ m pore, 12 mm polycarbonate filter (Millicell Merck Millipore, catalog no. PIH01250) suspended inside a cell culture well containing 500  $\mu$ L of 1x PBS. The epidermis was kept facing up. The TEER was measured immediately using the Millicell® ERS-2 Voltohmmeter (Millipore, catalog no. MERS00002).

In vitro TEER measurement was performed following the protocol described in reference.<sup>15</sup> Briefly, 40000 cells were seeded onto a 0.4  $\mu$ m pore, 12 mm polycarbonate filter suspended inside a cell culture well. After 24 hours, 500  $\mu$ L of solution containing the appropriate concentration of glucose were added. The TEER was measured with the Millicell® ERS-2 every 12 hours for 2 d against a blank well containing no cells.

### **MTT viability assay**

An MTT assay was performed using the MTT Cell Count Kit (Nacalai Tesque, catalog no. 23506-80) following the manufacturer's specifications. Briefly, 10000 cells were seeded in a 96 well dish and left to incubate for 48 h. The medium was replaced to phenol free D-MEM containing the correct concentration of glucose, and cells were again left to incubate for 48 h. Following this, 10  $\mu$ L of MTT (3-(4,5-dimethylthiazol-2-yl)-2,5-diphenyltetrazolium bromide) was pipetted into each well before incubating the plate for 3 hours at 37°C and at controlled CO<sub>2</sub> concentrations. The reaction was stopped with 100  $\mu$ L of acidified isopropanol (0.04 M HCl in absolute isopropanol), and a colorimetric reading was taken at 595 nm.

### **TUNEL**

Apoptosis was evaluated using the In Situ Cell Death Detection Kit Fluorescein (Roche, 11684795910). Briefly, 40000 cells were seeded overnight before being incubated with the appropriate concentrations of glucose for 48 h. Following this, the cells were fixed for 1 hour in 4% paraformaldehyde, rinsed with 1x PBS, permeabilized with 0.1% Triton® X-100 for 2 minutes, washed once more with 1x PBS and finally incubated with 50 $\mu$ L of TUNEL reaction mix for 1 hour at 37°C X in the dark. After this, the cells were washed with 1x PBS and mounted with VECTASHIELD antifade mounting medium with DAPI (Vector Laboratories, catalog no. H-1200) onto 18 mm square glasses. Treatment with 1000  $\mu$ M H<sub>2</sub>O<sub>2</sub> for 2 hours was used as positive control.

### **Osmolarity measurement**

15  $\mu$ L of medium, supernatant or serum were pipetted into cryosensitive tubes. An osmolarity measurement was taken using the Fiske One-Ten Osmometer (Fiske Associates, 110). 250 mM Mannitol and 15% HCl were used as positive and negative controls respectively.

### **Statistical analysis**

For all values, mean and standard error of mean (SEM) were calculated. Results are presented as mean  $\pm$  SEM. Statistical analyses were performed using an unpaired Student's t-test (when comparing 2 groups) or ANOVA (for the comparison of more than 2



groups). Post hoc tests were also performed. Statistical significance was set at  $p < 0.05$ . All statistics were calculated using Prism (Graphpad Software).

## Results

### Mouse model of type 2 diabetes

During the experimental protocol, WT and BLT2 knockout mice showed a similar weight gain in response to a HF or LF diet. From the third week onwards, a significant difference ( $p < 0.01$ ) in WT and BLT2 knockout mice was observed in the HF compared with LF group (Fig. 1).

Biochemical and metabolic parameters (Table 1) show that BLT2 knockout mice present higher basal glucose compared with WT animals on a controlled diet. This was increased by the HF diet. Moreover, the glucose levels of knockout mice on a LF diet are comparable to those of WT mice on a HF diet. Additionally, BLT2 knockouts had increased insulin levels as well as increased HOMA-IR and HOMA- $\beta$ . WT and BLT2 knockout mice both presented higher triglyceride levels in response to the HF diet ( $p < 0.05$ ), and a tendency ( $p = 0.07$ ) in the increase on total cholesterol levels.

The glucose tolerance test revealed a greater increase in blood glucose in BLT2 knockout mice than in the WT. However, the HF diet induced the classical glucose kinetics of diabetes (Fig. 2A). The

quantification of AUC showed these differences, confirming a sustained hyperglycemia (Fig. 2B).

### Skin structure and electric resistance in T2D WT and knockout mice

The skin histology of BLT2 knockout and T2D WT mice suggested an atrophic epidermis without signs of inflammatory cell infiltration or vasculitis (Fig. 3A). The quantification showed that, under a LF diet, the deletion of the *Ltb4r2* gene reduced the epidermal thickness ( $p < 0.01$ ) to a level comparable to control animals on a HF diet. This effect was more pronounced in the BLT2 knockout T2D mice (Fig. 3B).

### Inflammatory, matrix degradation and differentiation markers in the skin

The skin of BLT2 knockout mice showed lower levels of IL-1 $\beta$  mRNA than that of the WT ( $p < 0.01$ ). A similar effect was observed in tissue from WT animals having undergone 5 weeks of a HF diet (Fig. 4A).

In contrast, the levels of CXCL2, MMP9 and FLG mRNA were significantly elevated ( $p < 0.05$ ) in the skin of BLT2 knockout mice. A similar effect was induced in the WT mice by the HF diet (Fig. 4B–C).

The other differentiation markers showed an increase (all  $p < 0.05$ ) in response to the HF diet in all mice; however, in the BLT2 knockout mice, Loricrin mRNA levels increased more dramatically over the 5 weeks during which the mice were subjected to the diet (Fig. 4E, F).

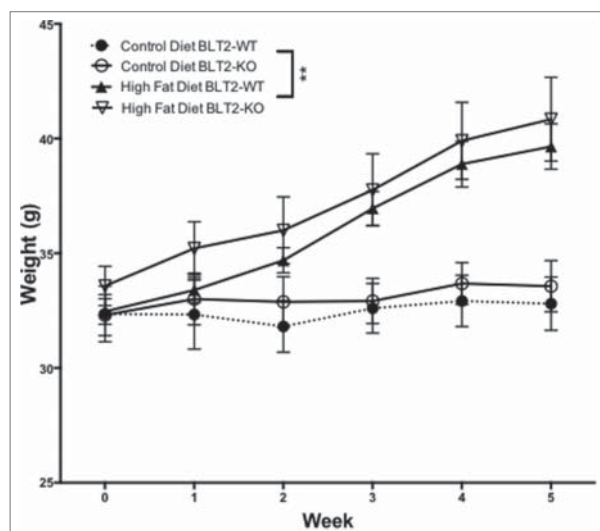


**Figure 1.** WT and BLT2 knockout mice show a similar trend in weight gain in response to control or high fat diet. Weekly weight measurements in non-sedated animals for 5 weeks (mean  $\pm$  SEM),  $n = 5$  per group  $**p < 0.01$  2-Way ANOVA.

### Cellular monolayer and transepithelial resistance

Under a low glucose concentration, the actin staining showed HaCaT-BLT2 cells to form an organized and compact monolayer. Cells that had been kept at 25 mM glucose for 48 h showed a disruption in the monolayer, which was more severe in cells that did not express BLT2 (Fig. 5A).

Additionally, BLT2 expressing cells had a higher TEER ( $p < 0.05$ ) compared with HaCaT-Mock cells at both low and high concentrations of glucose, although a 48 h exposure to high glucose concentrations led to a reduction in TEER in both cell lines ( $p < 0.05$ ; Fig. 5B).

Neither cellular viability nor induced apoptosis were impacted by 48 h at high glucose concentrations (Fig. S1A–B). Glucose concentrations did not alter the osmolarity of the treated medium or the supernatant after 48 hours (Fig. S1C).

**Table 1.** Metabolic and biochemical characteristics after 5 weeks of controlled diet (average  $\pm$  SEM),  $n = 5$  per group, \* or  $\S$   $p < 0.05$ , \*\* or ¶¶ or §§  $p < 0.01$  non parametric one-way ANOVA with Tukey's post hoc test.

| Biochemical Characteristics | Low Fat BLT2-WT  | Low Fat BLT2-KO   | High Fat BLT2-WT   | High Fat BLT2-KO   |
|-----------------------------|------------------|-------------------|--------------------|--------------------|
| Basal Glucose (mg/dL)       | 95.8 $\pm$ 4.7   | 139.2 $\pm$ 8.2** | 146.5 $\pm$ 9.6**  | 167.6 $\pm$ 15.5** |
| Insulin ( $\mu$ g/L)        | 0.82 $\pm$ 0.1   | 1.12 $\pm$ 0.1    | 2.08 $\pm$ 0.2**   | 3.50 $\pm$ 0.5§§   |
| HOMA-IR                     | 0.1 $\pm$ 0.02   | 0.3 $\pm$ 0.07*   | 0.7 $\pm$ 0.12§§   | 1.4 $\pm$ 0.23¶¶   |
| HOMA- $\beta$               | 145.4 $\pm$ 25.8 | 79.9 $\pm$ 14.2*  | 129.1 $\pm$ 14.2   | 195.3 $\pm$ 38.7§  |
| Cholesterol (mg/dL)         | 141 $\pm$ 18.2   | 138.2 $\pm$ 23.1  | 198.5 $\pm$ 15.77  | 197.2 $\pm$ 16.62  |
| Triglycerides (mg/dL)       | 85.8 $\pm$ 6.3   | 90 $\pm$ 12.1     | 136.2 $\pm$ 13.5** | 148.4 $\pm$ 14.12* |

### Wound healing and glucose concentrations in HaCaT cells

Compared to Mock cells, HaCaT-BLT2 cells showed an accelerated wound healing capacity in low glucose concentrations. High glucose concentrations reduced this capacity in both cell types; however, BLT2 expression improved wound healing even in high concentrations of glucose (all  $p < 0.01$ ; Fig. 6A–B).

### Inflammatory, matrix degradation and differentiation markers in cells

Consistent with the results obtained in skin, BLT2 expressing cells presented higher levels of IL-1 $\beta$  compared with Mock cells, and 48 h exposure to high concentrations of glucose significantly reduced IL-1 $\beta$  mRNA levels ( $p < 0.05$ ; Fig. 7A). Additionally, HaCaT-BLT2 cells showed lower levels of IL-8, MMP9, FLG, LOR and KRT10 mRNA compared with Mock cells ( $p < 0.05$ ). 48 h exposure to 25 mM glucose increased the levels of IL-8, MMP9, LOR and KRT10 mRNA; however, this increase is attenuated in BLT2-expressing cells (Fig. 7B–F).

### Discussion

We combined in vitro and in vivo approaches to investigate the role of the GPCR BLT2 in maintaining skin integrity in T2D by using an induced mouse model of T2D and a selective expression in vitro system. The main finding of our study is that BLT2 expression reduces the damaging effects of high glucose on the skin. In older diabetic mice, BLT2 deficiency increased epidermal atrophy, as well as reducing the TEER and altering the levels of various markers of inflammation (IL-1 $\beta$  and IL-8), matrix degradation (MMP9) and differentiation (FLG, LOR, KRT10). In addition, our results suggest that BLT2 knockout mice exhibit a spontaneous insulin resistance. In vitro, the absence of BLT2 disrupts the cellular monolayer, affecting its electric resistance and wound healing capacity, as well as dysregulating the levels of the markers of inflammation, matrix degradation and differentiation mentioned above. In line with this, BLT2-expressing cells are somewhat protected from the negative effects of glucose, and a better functionality is observed in these cells.

The use of a non-genetic, induced, murine T2D model represents an important novelty in the context of the

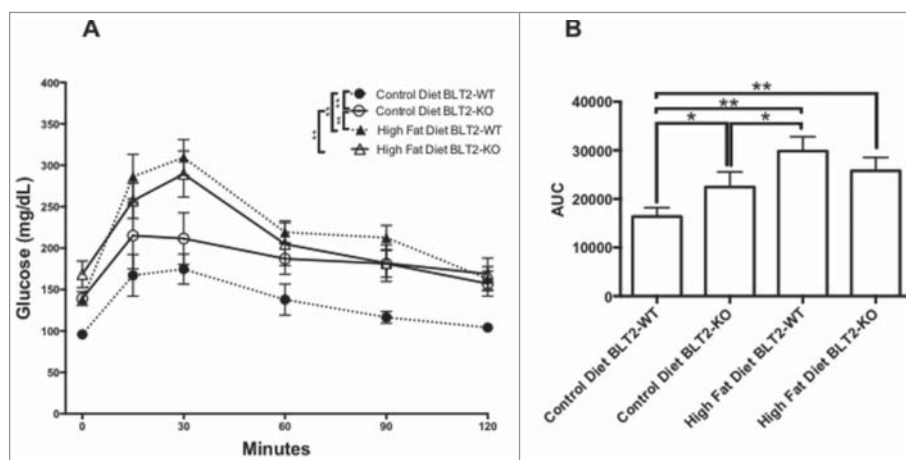


**Figure 2.** BLT2 knockout mice show an abrogated glucose response, sign of spontaneous T2D. (A) Glucose tolerance test after 5 weeks of controlled diet in WT and knockout mice, 6 measurements were taken after 1 g/kg glucose IP injection (mean  $\pm$  SEM).  $n = 5$  animals per group \*\* $p < 0.01$  2-Way ANOVA. (B) Area under the glucose tolerance test curves (mean  $\pm$  SEM).  $n = 5$  animals per group \* $p < 0.05$  \*\* $p < 0.01$ , non-parametric One-Way ANOVA with Tukey's post hoc test.

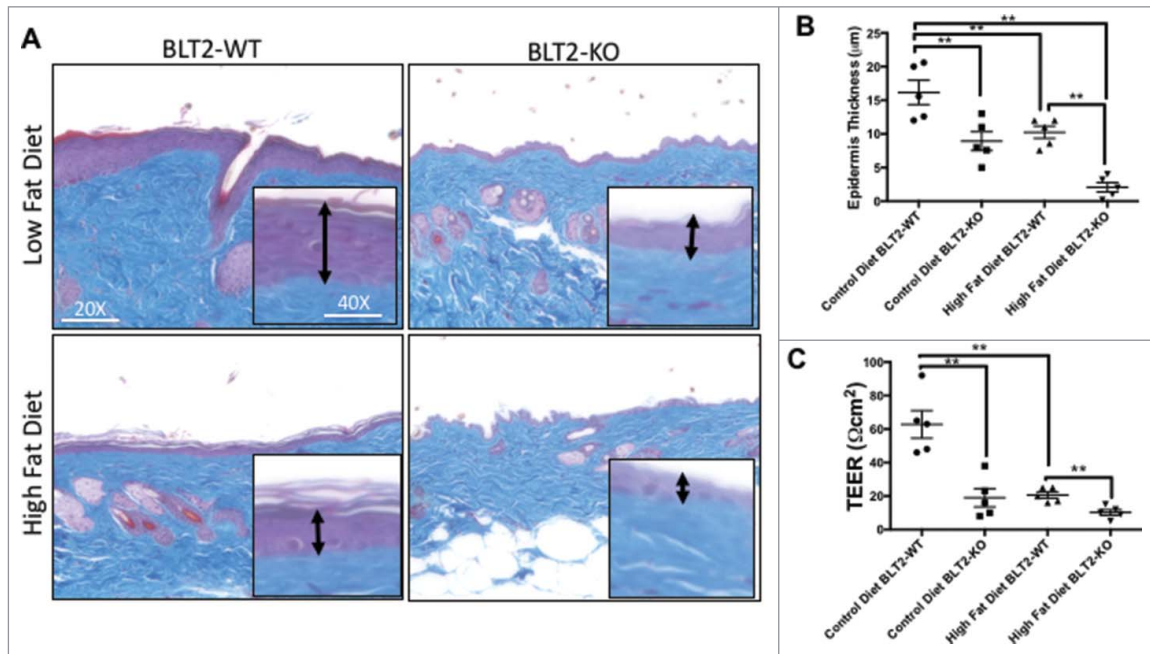


**Figure 3.** The skin from BLT2 KO and T2D mice present atrophic epidermis and reduced TEER. (A) Microphotographs MT stains at 20x magnification and representative insets at double magnification, (B) semi-quantification of epidermal thickness and (C) *Ex vivo* TEER. The data shown represent the mean  $\pm$  SEM,  $n = 5$  animals per group \*\*\* $p < 0.01$ , non-parametric One-Way ANOVA with Tukey's post hoc test.

results obtained in this study. Various reports have validated the use of a HF diet over several weeks to provide a model of T2D, as well as the evaluation of weight, glucose

tolerance and insulin levels as main pathologically indicative parameters.<sup>24-26</sup> This strategy allowed the proper study of the BLT2 deletion, optimizing the sample size

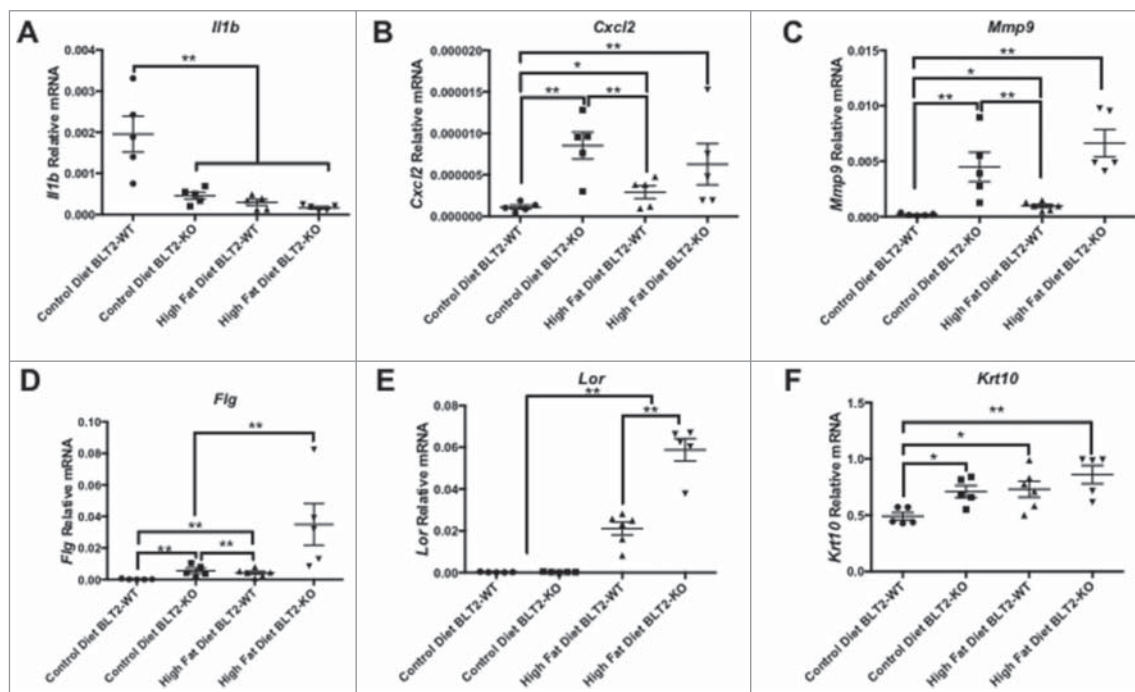


**Figure 4.** The skin from BLT2 knockout mice exhibits increased levels of inflammatory, matrix degradation and differentiation markers compared with tissue from T2D animals. Q-PCR for (A) *Il1b*, (B) *Cxcl2*, (C) *Mmp9*, (D) *Flg*, (E) *Lor* and (F) *Krt10*, relative to *actb* in skin from WT and BLT2 knockout mice under control or high fat diet for 5 weeks. Data represent the mean  $\pm$  SEM of  $n = 5$  per group, \* $p < 0.05$  \*\* $p < 0.01$  non-parametric One-Way ANOVA with Tukey's post hoc test.

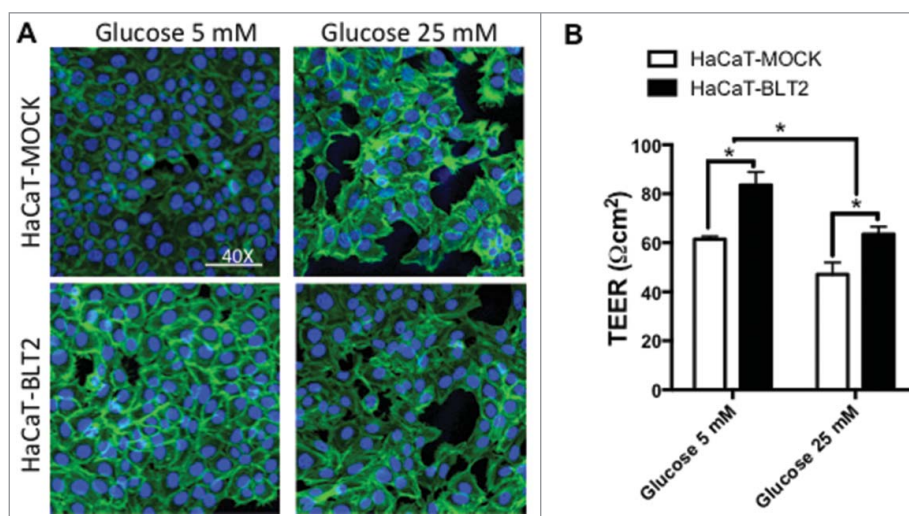


**Figure 5.** High glucose levels disorganize the actin structure disrupting the monolayer and reducing the TEER in HaCaT cells, an alteration that is prevented by BLT2 expression. (A) Representative confocal microphotographs of actin fluorescence stain (Phalloidin-FITC) in HaCaT cells after 48 h under low (5 mM) and high (25 mM) glucose levels. In blue: nucleus stain by DAPI.  $n = 3$  independent experiments. (B) Transepithelial resistance (TEER) assay in high or low glucose levels after 48 h. Data represent the mean  $\pm$  SEM of  $n = 3$  independent experiments \* $p < 0.05$  non parametric One-Way ANOVA with Tukey's post hoc test.

and ensuring limited data dispersion for the application of the appropriate statistical tests.

Unexpectedly, the BLT2 knockout mice showed signs of spontaneous diabetes without an obese phenotype. The skin alterations observed in these animals could be partially attributed to the hyperglycemia. Further studies are required to elucidate the participation of the GPCR BLT2 in glucose metabolism.

Interestingly, it has been reported that LTB<sub>4</sub>, a low affinity ligand for BLT2 and high affinity ligand for

BLT1, promotes the migration of monocytes into adipose tissue, thereby activating proinflammatory pathways<sup>27</sup> and acting as a major driver of insulin resistance in obese mice. Moreover, BLT1 deficiency protects against systemic insulin resistance in response to obesity.<sup>28</sup> More studies are required to evaluate whether BLT2 participation in the regulation of glucose metabolism is part of a complementary or a parallel pathway.

Few studies to date have investigated the pathological state of the skin in T2D. Most of these studies have found

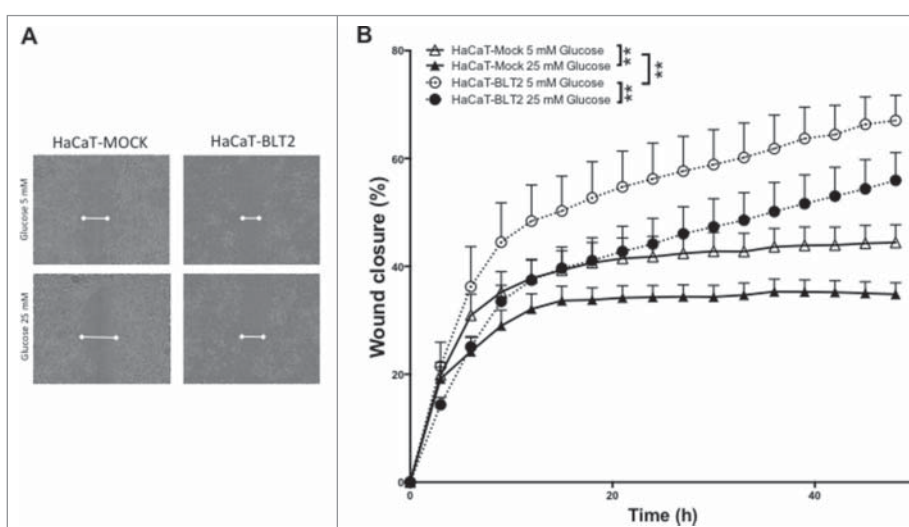


**Figure 6.** High glucose reduces wound healing capacity, an effect that is attenuated in cells that express BLT2. (A) Representative microphotographs of wound healing assays in HaCaT cells, for 48 h under low (5 mM) and high (25 mM) glucose, (B) typical kinetic curve of migration and wound closure. Data represent the mean  $\pm$  SEM,  $n = 6$  independent experiments \*\* $p < 0.01$  2-Way ANOVA.



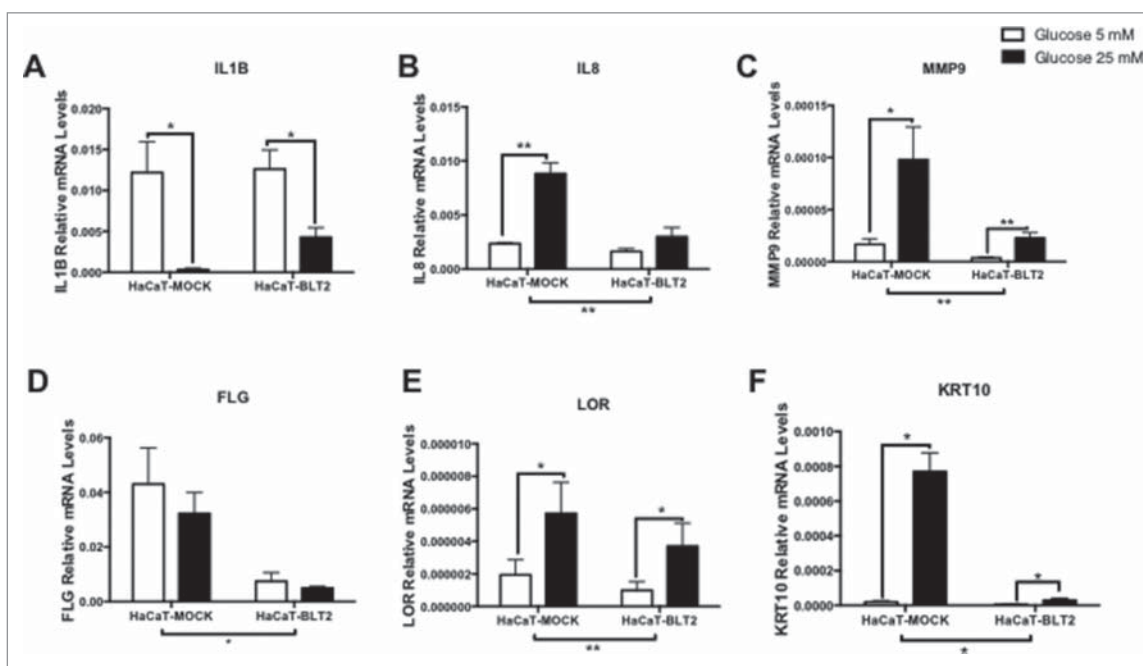


**Figure 7.** Cells that do not express BLT2 present altered levels of inflammatory, matrix degradation and differentiation markers. High glucose exerts a more severe effect on these cells. Q-PCR for *IL1B*, *IL8*, *MMP9*, *FLG*, *LOR* and *KRT10* relative to *ACTB*, in HaCaT Mock and BLT2 after 48 h of low (5 mM) or high (25 mM) glucose. Data represent the mean  $\pm$  SEM,  $n = 3$  independent experiments run in duplicate \* $p < 0.05$  \*\* $p < 0.01$  non-parametric One-Way ANOVA with Tukey's post hoc test.

that affected animals present delayed wound healing, altered MCP-1 levels and a disorganized epidermal structure. In addition, cyclooxygenase (COX)-1 and -2 expression and activity have been found to be severely dysregulated in chronically obese ob/ob mice.<sup>29,30</sup>

Even though skin problems represent a highly documented complication, which is driven by the protein glycosylation caused by chronic non treated T2D,<sup>31</sup> and although advances in proteome technologies are allowing the identification of molecular alterations in the tissue,<sup>32</sup> this study is the first to demonstrate that, under the pathological conditions of T2D, the skin exhibits a reduction in epidermal thickness, TEER, a downregulation of *Il1b* expression, and an upregulation of *Cxcl2*, *Mmp9*, *Flg*, *Lor* and *Krt10*. Considering that BLT2 deficiency enhances the observed changes in the skin, our results furthermore suggest a role for BLT2 in modulating all of the observed parameters.

When researching diabetes in vitro, it is established to model normoglycemic conditions at around 5 mM glucose (eq. 90 mg/dL) and hyperglycemia at 25 mM (eq. 450 mg/dL). This is based on the finding of morphological and functional alterations emulating diabetes after 24 h of culture under these high glucose conditions.<sup>33-35</sup> Even though only a small number of animals reached such high glucose levels during the tolerance test, it is

accepted to use the concentration of 25 mM to mimic the pathological conditions of T2D, a use that is not limited to keratinocyte research.<sup>36</sup>

It has been reported that high glucose levels induce a reduction of the expression of *IL1B*,<sup>37</sup> an important pro-regenerative cytokine,<sup>38</sup> while increasing *IL8* levels,<sup>35</sup> mediating the upregulation of *MMP9*<sup>39</sup> and the differentiation process,<sup>33</sup> causing impaired wound healing<sup>40,41</sup> as well as epithelial barrier damage.<sup>42,43,45</sup> Nonetheless, this is the first study that uses a HaCaT model to show that these alterations are regulated by BLT2 expression, and that this is the effect of this receptor to attenuate the negative effect of the high glucose concentrations.

Importantly, previous reports linking the 12-HHT/BLT2 axis to type 1 diabetes wound healing impairments have studied its activation and endogenous modulation by pharmacological ligands, not the effect of expression itself. Moreover, it has been reported that human keratinocytes lack the components to produce endogenous LTB4 and 12-HHT,<sup>44</sup> supporting that the results obtained in vitro are attributable to BLT2 expression and not to its activation.

The terminal differentiation of keratinocytes is characterized by cellular changes associated with apoptosis.<sup>45</sup> This process begins when the transient amplifying cells

withdraw from the cell cycle and lose their ability to adhere to the basement membrane zone, reducing the cellular metabolic activity.<sup>46</sup> Reports show that high concentrations of glucose lead to an increase in the levels of the classic differentiation markers FLG, LOR<sup>47,48</sup> and K10.<sup>33,49</sup> Moreover, it has been suggested that the regulated expression of FLG modulates monolayer integrity, cell-cell adhesion and cell cycle arrest.<sup>50</sup> The results obtained in this study are in concordance with the literature, showing that these 3 markers are upregulated under high glucose concentrations *in vitro* and *in vivo*. The mitigating effect of BLT2 expression on processes involved in terminal differentiation is a finding, which has never been reported before, and which could partly explain the protective capacity of the BLT2 receptor and the enhanced wound healing capacity presented by the cells expressing it.

Although more experiments are needed to understand the protective mechanism of BLT2 in keratinocytes, our results complement previous reports and open the possibilities for future clinical studies on wound healing management using topic preparations of BLT2 ligand analogs that are currently in development in the pharmaceutical industry.

It has been shown that insulin resistance can start from an early age,<sup>51</sup> thereby increasing the predisposition for complications associated with diabetes in the later years of life. The clinical management of the complications of T2D is therefore an important public health issue; more work on this topic is required in the future.

### Disclosure of potential conflicts of interest

No potential conflicts of interest were disclosed.

### Acknowledgments

This work was supported by the Ministry of Education, Culture, Sports, Science and Technology of Japan grants to the Biochemistry 1 laboratory where this work was executed. Part of these results were presented at the Research presentations of the Institute for Disease of Old Age held in March 17th, 2015 at Juntendo University.

The author also thanks to Dr T. Yokomizo for the mentorship and Drs T. Koga and K. Saeki for the technical and intellectual support.

### Funding

ALR was supported as post doctoral fellow by the Research Institute for Disease of Old Age.

### ORCID

Alberto Leguina-Ruzzi  <http://orcid.org/0000-0002-4761-3491>

Juan P. Valderas  <http://orcid.org/0000-0001-8508-3340>

### References

- [1] World Health Statistics, WHO. 2015. [accessed 2016 Oct 3]. [www.who.int/gho/publications/world\\_health\\_statistics/2015/en/](http://www.who.int/gho/publications/world_health_statistics/2015/en/)
- [2] Paneni F, Costantino S, Cosentino F. Molecular mechanism of vascular dysfunction and cardiovascular biomarkers in type 2 diabetes. *Cardiovasc Diagn Ther* 2014; 4(4):324-32; PMID:25276618
- [3] Fonseca VA. Defining and characterizing the progression of type 2 diabetes. *Diabetes Care* 2009; 32(Suppl 2):S151-6; PMID:19875543; <http://dx.doi.org/10.2337/dc09-S301>
- [4] Muller IS, de Grauw WJ, van Gerwen WH, Bartelink ML, van Den Hoogen HJ, Rutten GE. Foot ulceration and lower limb amputation in type 2 diabetic patients in dutch primary health care. *Diabetes Care* 2002; 25(3):570-4; PMID:11874949; <http://dx.doi.org/10.2337/diacare.25.3.570>
- [5] Kamohara M, Takasaki J, Matsumoto M, Saito T, Ohishi T, Ishii H, Furuichi K. Molecular cloning and characterization of another leukotriene B4 receptor. *J Biol Chem* 2000; 275(35):27000-4; PMID:10889186
- [6] Yokomizo T, Kato K, Hagiya H, Izumi T, Shimizu T. Hydroxyeicosanoids bind to and activate the low affinity leukotriene B4 receptor, BLT2. *J Biol Chem* 2001; 276(15):12454-9; PMID:11278893; <http://dx.doi.org/10.1074/jbc.M011361200>
- [7] Liu M, Saeki K, Matsunobu T, Okuno T, Koga T, Sugimoto Y, Yokoyama C, Nakamizo S, Kabashima K, Narumiya S, et al. 12-Hydroxyheptadecatrienoic acid promotes epidermal wound healing by accelerating keratinocyte migration via the BLT2 receptor. *J Exp Med* 2014; 211(6):1063-78; PMID:24821912; <http://dx.doi.org/10.1084/jem.20132063>
- [8] Iizuka Y, Yokomizo T, Terawaki K, Komine M, Tamaki K, Shimizu T. Characterization of a mouse second leukotriene B4 receptor, mBLT2: BLT2-dependent ERK activation and cell migration of primary mouse keratinocytes. *J Biol Chem* 2005; 280(26):24816-23; PMID:15866883; <http://dx.doi.org/10.1074/jbc.M413257200>
- [9] Yoo MH, Song H, Woo CH, Kim H, Kim JH. Role of the BLT2, a leukotriene B4 receptor, in Ras transformation. *Oncogene* 2004; 23(57):9259-68; PMID:15489890
- [10] Hennig R, Osman T, Esposito I, Giese N, Rao SM, Ding XZ, Tong WG, Büchler MW, Yokomizo T, Friess H, et al. BLT2 is expressed in PanINs, IPMNs, pancreatic cancer and stimulates tumour cell proliferation. *Br J Cancer* 2008; 99(7):1064-73; PMID:18781173; <http://dx.doi.org/10.1038/sj.bjc.6604655>
- [11] Shao WH, Del Prete A, Bock CB, Haribabu B. Targeted disruption of leukotriene B4 receptors BLT1 and BLT2: a critical role for BLT1 in collagen-induced arthritis in mice.

- J Immunol 2006; 176(10):6254-61; PMID:16670336; <http://dx.doi.org/10.4049/jimmunol.176.10.6254>
- [12] Cho KJ, Seo JM, Shin Y, Yoo MH, Park CS, Lee SH, Chang YS, Cho SH, Kim JH. Blockade of airway inflammation and hyperresponsiveness by inhibition of BLT2, a low-affinity leukotriene B4 receptor. *Am J Respir Cell Mol Biol* 2010; 42(3):294-303; PMID:19448154; <http://dx.doi.org/10.1165/rcmb.2008-0445OC>
- [13] Matsunaga Y, Fukuyama S, Okuno T, Sasaki F, Matsunobu T, Asai Y, Matsumoto K, Saeki K, Oike M, Sadamura Y, et al. Leukotriene B4 receptor BLT2 negatively regulates allergic airway eosinophilia. *FASEB J* 2013; 27(8):3306-14; PMID:23603839; <http://dx.doi.org/10.1096/fj.12-217000>
- [14] Iizuka Y, Okuno T, Saeki K, Uozaki H, Okada S, Misaka T, Sato T, Toh H, Fukayama M, Takeda N, et al. Protective role of the leukotriene B4 receptor BLT2 in murine inflammatory colitis. *FASEB J* 2010; 24(12):4678-90; PMID:20667973; <http://dx.doi.org/10.1096/fj.10-165050>
- [15] Ishii Y, Saeki K, Liu M, Sasaki F, Koga T, Kitajima K, Meno C, Okuno T, Yokomizo T. Leukotriene B4 receptor type 2 (BLT2) enhances skin barrier function by regulating tight junction proteins. *FASEB J* 2016; 30(2):933-47; PMID:26527063; <http://dx.doi.org/10.1096/fj.15-279653>
- [16] Chiba T, Nakahara T, Hashimoto-Hachiya A, Yokomizo T, Uchi H, Furue M. The leukotriene B4 receptor BLT2 protects barrier function via actin polymerization with phosphorylation of myosin phosphatase target subunit 1 in human keratinocytes. *Exp Dermatol* 2016; 25(7):532-6; PMID:26896822; <http://dx.doi.org/10.1111/exd.12976>
- [17] Luo L, Tanaka R, Kanazawa S, Lu F, Hayashi A, Yokomizo T, Mizuno H. A synthetic leukotriene B4 receptor type 2 agonist accelerates the cutaneous wound healing process in diabetic rats by indirect stimulation of fibroblasts and direct stimulation of keratinocytes. *J Diabetes Complications* 2016; S1056-8727(16):30541-4
- [18] Wikramanayake TC, Stojadinovic O, Tomic-Canic M. Epidermal Differentiation in Barrier Maintenance and Wound Healing. *Adv Wound Care (New Rochelle)* 2014; 3(3):272-280; PMID:24669361; <http://dx.doi.org/10.1089/wound.2013.0503>
- [19] Kabashima K, Murata T, Tanaka H, Matsuoka T, Sakata D, Yoshida N, Katagiri K, Kinashi T, Tanaka T, Miyasaka M, et al. Thromboxane A2 modulates interaction of dendritic cells and T cells and regulates acquired immunity. *Nat Immunol* 2003; 4(7):694-701; PMID:12778172; <http://dx.doi.org/10.1038/ni943>
- [20] Terawaki K, Yokomizo T, Nagase T, Toda A, Taniguchi M, Hashizume K, Yagi T, Shimizu T. Absence of leukotriene B4 receptor 1 confers resistance to airway hyperresponsiveness and Th2-type immune responses. *J Immunol* 2005; 175(7):4217-25; PMID:16177061; <http://dx.doi.org/10.4049/jimmunol.175.7.4217>
- [21] Matsunobu T, Okuno T, Yokoyama C, Yokomizo T. Thromboxane A synthase-independent production of 12-hydroxyheptadecatrienoic acid, a BLT2 ligand. *J Lipid Res* 2013; 54(11):2979-87; PMID:24009185; <http://dx.doi.org/10.1194/jlr.M037754>
- [22] Sasaki F, Okuno T, Saeki K, Min L, Onohara N, Kato H, Shimizu T, Yokomizo T. A high-affinity monoclonal antibody against the FLAG tag useful for G-protein-coupled receptor study. *Anal Biochem* 2012; 425(2):157-65; PMID:22465329; <http://dx.doi.org/10.1016/j.ab.2012.03.014>
- [23] Kuo IH, Carpenter-Mendini A, Yoshida T, McGirt LY, Ivanov AI, Barnes KC, Gallo RL, Borkowski AW, Yamasaki K, Leung DY, et al. Activation of epidermal toll-like receptor 2 enhances tight junction function: implications for atopic dermatitis and skin barrier repair. *J Invest Dermatol* 2013; 133(4):988-98; PMID:23223142; <http://dx.doi.org/10.1038/jid.2012.437>
- [24] Winzell MS, Ahrén B. The high-fat diet-fed mouse: a model for studying mechanisms and treatment of impaired glucose tolerance and type 2 diabetes. *Diabetes* 2004; 53(Suppl 3):S215-9; PMID:15561913; [http://dx.doi.org/10.2337/diabetes.53.suppl\\_3.S215](http://dx.doi.org/10.2337/diabetes.53.suppl_3.S215)
- [25] King AJ. The use of animal models in diabetes research. *Br J Pharmacol* 2012; 166(3):877-94; PMID:22352879; <http://dx.doi.org/10.1111/j.1476-5381.2012.01911.x>
- [26] Gilbert ER, Fu Z, Liu D. Development of a nongenetic mouse model of type 2 diabetes. *Exp Diabetes Res* 2011; 2011:416254; PMID:22164157; <http://dx.doi.org/10.1155/2011/416254>
- [27] Li P, Oh DY, Bandyopadhyay G, Lagakos WS, Talukdar S, Osborn O, Johnson A, Chung H, Mayoral R, Maris M, et al. LTB4 promotes insulin resistance in obese mice by acting on macrophages, hepatocytes and myocytes. *Nat Med* 2015; 21(3):239-47; PMID:25706874
- [28] Fouda MM, Abdel-Mohsen AM, Ebaid H, Hassan I, Al-Tamimi J, Abdel-Rahman RM, Metwalli A, Alhazza I, Rady A, El-Faham A, et al. Deficiency of the leukotriene B4 receptor, BLT-1, protects against systemic insulin resistance in diet-induced obesity. *Int J Biol Macromol* 2016; 89:582-91; PMID:27174907; <http://dx.doi.org/10.1016/j.ijbiomac.2016.05.021>
- [29] Desposito D, Chollet C1, Taveau C, Descamps V, Alhenc-Gelas F, Roussel R, Bouby N, Waeckel L. Improvement of skin wound healing in diabetic mice by kinin B2 receptor blockade. *Clin Sci (Lond)* 2016; 130(1):45-56; PMID:26443866; <http://dx.doi.org/10.1042/CS20150295>
- [30] Kämpfer H, Schmidt R, Geisslinger G, Pfeilschifter J, Frank S. Wound inflammation in diabetic ob/ob mice: functional coupling of prostaglandin biosynthesis to cyclooxygenase-1 activity in diabetes-impaired wound healing. *Diabetes* 2005; 54(5):1543-51; <http://dx.doi.org/10.2337/diabetes.54.5.1543>
- [31] Brownlee M. Advanced protein glycosylation in diabetes and aging. *Annu Rev Med* 1995; 46:223-34; PMID:7598459; <http://dx.doi.org/10.1146/annurev.med.46.1.223>
- [32] List EO, Berryman DE, Palmer AJ, Qiu L, Sankaran S, Kohn DT, Kelder B, Okada S, Kopchick JJ. Analysis of mouse skin reveals proteins that are altered in a diet-induced diabetic state: a new method for detection of type 2 diabetes. *Proteomics* 2007; 7(7):1140-9; PMID:17390296; <http://dx.doi.org/10.1002/pmic.200600641>
- [33] Spravchikov N, Sizyakov G, Gartsbein M, Accili D, Tennenbaum T, Wertheimer E. Glucose effects on skin

- keratinocytes: implications for diabetes skin complications. *Diabetes* 2001; 50(7):1627-35; PMID:11423485; <http://dx.doi.org/10.2337/diabetes.50.7.1627>
- [34] Terashi H, Izumi K, Deveci M, Rhodes LM, Marcelo CL. High glucose inhibits human epidermal keratinocyte proliferation for cellular studies on diabetes mellitus. *Int Wound J* 2005; 2(4):298-304; PMID:16618316; <http://dx.doi.org/10.1111/j.1742-4801.2005.00148.x>
- [35] Lan CC, Wu CS, Huang SM, Wu IH, Chen GS. High-glucose environment enhanced oxidative stress and increased interleukin-8 secretion from keratinocytes: new insights into impaired diabetic wound healing. *Diabetes* 2013; 62(7):2530-8; PMID:23423570; <http://dx.doi.org/10.2337/db12-1714>
- [36] Reed MJ, Scribner KA. In-vivo and in-vitro models of type 2 diabetes in pharmaceutical drug discovery. *Diabetes Obes Metab* 1999; 1(2):75-86; PMID:11220515; <http://dx.doi.org/10.1046/j.1463-1326.1999.00014.x>
- [37] Salpea KD, Maubaret CG, Kathagen A, Ken-Dror G, Gilroy DW, Humphries SE. The effect of pro-inflammatory conditioning and/or high glucose on telomere shortening of aging fibroblasts. *PLoS One* 2013; 8(9):e73756; PMID:24086293; <http://dx.doi.org/10.1371/journal.pone.0073756>
- [38] Rozlomiy VL, Markov AG. Effect of interleukin-1 $\beta$  on the expression of tight junction proteins in the culture of HaCaT keratinocytes. *Bull Exp Biol Med* 2010; 149(3):280-3; PMID:21246082; <http://dx.doi.org/10.1007/s10517-010-0927-y>
- [39] Tsai WC, Liang FC, Cheng JW, Lin LP, Chang SC, Chen HH, Pang JH. High glucose concentration up-regulates the expression of matrix metalloproteinase-9 and -13 in tendon cells. *BMC Musculoskelet Disord* 2013; 14:255; PMID:23981230; <http://dx.doi.org/10.1186/1471-2474-14-255>
- [40] Lan CC, Liu IH, Fang AH, Wen CH, Wu CS. Hyperglycaemic conditions decrease cultured keratinocyte mobility: implications for impaired wound healing in patients with diabetes. *Br J Dermatol* 2008; 159(5):1103-15; PMID:18717678
- [41] Pan F, Guo R, Cheng W, Chai L, Wang W, Cao C, Li S. High glucose inhibits ClC-2 chloride channels and attenuates cell migration of rat keratinocytes. *Drug Des Devel Ther* 2015; 9:4779-91; PMID:26355894
- [42] Pavan B, Capuzzo A2, Forlani G. High glucose-induced barrier impairment of human retinal pigment epithelium is ameliorated by treatment with Goji berry extracts through modulation of cAMP levels. *Exp Eye Res* 2014; 120:50-4; PMID:24345371; <http://dx.doi.org/10.1016/j.exer.2013.12.006>
- [43] Qing Q, Zhang S, Chen Y, Li R, Mao H, Chen Q. High glucose-induced intestinal epithelial barrier damage is aggravated by syndecan-1 destruction and heparanase overexpression. *J Cell Mol Med* 2015; 19(6):1366-74; PMID:25702768; <http://dx.doi.org/10.1111/jcmm.12523>
- [44] Breton J, Woolf D, Young P, Chabot-Fletcher M. Human keratinocytes lack the components to produce leukotriene B<sub>4</sub>. *J Invest Dermatol* 1996; 106(1):162-7; PMID:8592068; <http://dx.doi.org/10.1111/1523-1747.ep12329890>
- [45] Allombert-Blaise C, Tamiji S, Mortier L, Fauvel H, Tual M, Delaporte E, Piette F, DeLassale EM, Formstecher P, Marchetti P, et al. Terminal differentiation of human epidermal keratinocytes involves mitochondria- and caspase-dependent cell death pathway. *Cell Death Differ* 2003; 10(7):850-2; PMID:12815468; <http://dx.doi.org/10.1038/sj.cdd.4401245>
- [46] Wikramanayake TC, Stojadinovic O, Tomic-Canic M. Epidermal differentiation in barrier maintenance and wound healing. *Adv Wound Care (New Rochelle)* 2014; 3(3):272-280; PMID:24669361; <http://dx.doi.org/10.1089/wound.2013.0503>
- [47] Thyssen JP, Linneberg A, Carlsen BC, Johansen JD, Engkilde K, Hansen T, Pociot F, Pedersen O, Meldgaard M, Szecsi PB, et al. A possible association between a dysfunctional skin barrier (filaggrin null-mutation status) and diabetes: a cross-sectional study. *BMJ Open* 2011; 1(1):e000062; PMID:22021744; <http://dx.doi.org/10.1136/bmjopen-2011-000062>
- [48] Nakahara T, Mitoma C, Hashimoto-Hachiya A, Takahara M, Tsuji G, Uchi H, Yan X, Hachisuka J, Chiba T, Esaki H, et al. Antioxidant *Opuntia ficus-indica* Extract Activates AHR-\NRF2 Signaling and Upregulates Filaggrin and Loricrin Expression in Human Keratinocytes. *J Med Food* 2015; 18(10):1143-9; PMID:26061570; <http://dx.doi.org/10.1089/jmf.2014.3396>
- [49] Wertheimer E, Spravchikov N, Trebicz M, Gartsbein M, Accili D, Avinoah I, Nofeh-Moses S, Sizyakov G, Tennenbaum T. The regulation of skin proliferation and differentiation in the IR null mouse: implications for skin complications of diabetes. *Endocrinology* 2001; 142(3):1234-41; PMID:11181540
- [50] Presland RB, Kuechle MK, Lewis SP, Fleckman P, Dale BA. Regulated expression of human filaggrin in keratinocytes results in cytoskeletal disruption, loss of cell-cell adhesion, and cell cycle arrest. *Exp Cell Res* 2001; 270(2):199-213; PMID:11640884; <http://dx.doi.org/10.1006/excr.2001.5348>
- [51] Leguina-Ruzzi A, Pereira J, Pereira-Flores K, Valderas JP, Mezzano D, Velarde V, Sáez CG. Increased RhoA/Rho-Kinase Activity and Markers of Endothelial Dysfunction in Young Adult Subjects with Metabolic Syndrome. *Metab Syndr Relat Disord* 2015; 13(9):373-80; PMID:26512756; <http://dx.doi.org/10.1089/met.2015.0061>